PROCEEDINGS OF SCIENCE

High-statistics CRPropa simulations for UHECR anisotropy studies

Simone Rossoni[a,*] **and Günter Sigl**[a]

[a] *II. Institute for Theoretical Physics, Universität Hamburg, Luruper Chaussee 149, 22761 Hamburg, Germany*

E-mail: simone.rossoni@desy.de, guenter.sigl@desy.de

Despite recent experimental evidence for an anisotropic component in the ultra-high-energy cosmic ray (UHECR) sky for energies above a few EeV, the nature and distribution of UHECR sources are still not well understood. Identification of cosmic particle accelerators in the sky is complicated by UHECR interactions with background photon fields and by the deflection in extragalactic and galactic magnetic fields (EGMF and GMF). Moreover, the spatial structure of the EGMF is not yet well understood, which makes the back-tracking of UHECRs a non-trivial task. In this work we study the propagation of UHECRs for a range of UHECR source distributions and EGMF models. We simulate extragalactic UHECR propagation and interactions by using the Monte Carlo code CRPropa3. UHECR deflection in the GMF is taken into account by mapping arrival directions at the edge of the Milky Way to those at Earth for particular GMF models. We then predict the anisotropy observables of the propagated UHECRs at Earth for various combinations of source catalogues, injected energy and mass distributions, and EGMF models. Based on this, the impact of the different model ingredients on the observables is discussed. Comparison with UHECR data will eventually allow us to put further constraints on scenarios for the source and EGMF distributions.

38th International Cosmic Ray Conference (ICRC2023)
26 July - 3 August, 2023
Nagoya, Japan

*Speaker

PoS(ICRC2023)433

1. Introduction

The most energetic particles ever observed in nature are not produced on Earth, they come from outside the solar system. However, the identification of the astrophysical sources capable of reaching such ultra-high-energy is still an open problem of modern particle and astroparticle physics. Nowadays we call these particles ultra-high-energy cosmic rays (UHECRs); they consist of ionized nuclei with energy greater than $\sim 10^{18}$ eV. These particles travel astrophysical distances in the galactic and extragalactic space before reaching cosmic ray observatories able to detect them.

The Pierre Auger Observatory [1] is the world's largest UHECR observatory: it measures the energy spectrum, the mass composition and the arrival directions of cosmic rays interacting with Earth's atmosphere up to $\sim 10^{20}$ eV. With regards to arrival directions of the observed UHECR, the data collected by the Auger Observatory has shown a dipole component in the UHECR sky above $8 \cdot 10^{18}$ eV [2] at $\sim 120°$ away from the Galactic Center. This observation shows that the UHECR sky is not purely isotropic, and suggests that UHECR sources may lie outside the Milky Way.

Despite the high quality of data collected by modern observatories, measuring the arrival directions of UHECRs does not provide direct information on the location of their sources. This is due to the presence of both cosmic background photon fields, galactic and extragalactic magnetic fields (GMF and EGMF). The induced magnetic deflection is proportional to the inverse of the rigidity $R = E/Z$ of the cosmic ray and, as these particles travel over astrophysical distances, the true position of the source may be hidden by the total deflection accumulated during the propagation. Another issue to be considered is that the strength and the 3D structure of the EGMF is not yet well known. Therefore, numerical replicas of our local Universe based on cosmological simulations are an important component for studying the impact that different magnetic field models might have on UHECR observables.

2. UHECR interactions and EGMF models

The propagation of ultra-high-energy particles through the extragalactic space depends on two effects: energy loss processes and magnetic deflections. These two mechanisms simultaneously affect the information we can obtain from the observation of UHECRs. Photohadronic interactions define the maximum distance we are able to observe when we only consider particles with energy above a specific value. At the same time, interactions can change the rigidity of the cosmic ray, thus modifying the expected magnetic deflection. The presence of an EGMF not only changes the arrival direction of a cosmic ray with respect to the line of sight of the source, but low energy particles emitted by distant sources could be deflected to such an extent that they would never reach the Earth (e.g. protons with energy $E = 8 \cdot 10^{18}$ eV coming from a source at 100 Mpc are deflected by $\theta \sim 40°$ by a magnetic field with $B_{\rm rms} = 1$ nG and $\lambda_{\rm c} = 1$ Mpc). The latter effect could give rise to a magnetic horizon that would further limit our maximum observable distance.

In this work, we simulate the propagation of UHECRs in the extragalactic space by taking into account the presence of cosmic background photon fields. We consider interactions with the Cosmic Microwave Background (CMB) [3, 4] and the Extragalactic Background Light (EBL). For the EBL we adopt the model [5]. We consider the production of electron-positron pairs, the production of

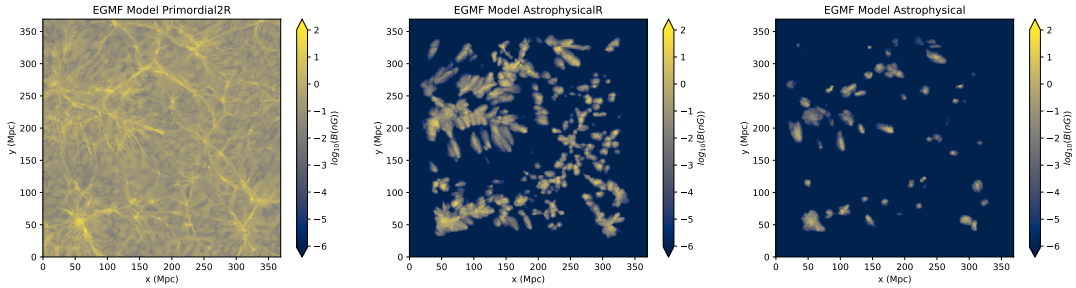

Figure 1: Magnetic field strength in nG in super-galactic coordinates at $z = 0$. The plots show the super-galactic plane orthogonal to the Z-axis including the Milky Way at the center. From left to right: models *primordial2R*, *astrophysicalR* and *astrophysical* from [7]. The color scale is expressed in $\log_{10}(B/1\,\mathrm{nG})$.

pions and the photodisintegration of heavy nuclei. The redshift energy loss due to expansion of the Universe and the nuclear decay of unstable nuclei are also taken into account in our simulations.

We want to investigate the impact of a realistic cosmic structure in the near Universe. For this purpose, we consider constrained MagnetoHydroDynamics (MHD) cosmological simulations that follow the evolution of the cosmic web. These simulations were obtained with the cosmological-grid-code ENZO [6]. An extensive discussion of the MHD simulations used in this work can be found in [7]: the numerical replica of our local Universe at $z = 0$ was obtained by initializing a simulation volume of $(500\,\mathrm{Mpc/h})^3$ at $z = 60$ with the Milky Way in the center, and following the evolution of cosmic structures (in this work $h = 0.677$). The evolution of the EGMF is simulated together with the matter density distribution.

In this work, we consider three structured EGMF models reported in [7]. In the *primordial2R* model, the EGMF is obtained from a power-law distribution with spectral index $n_B = -3$ at $z = 60$. The normalization of the *primordial2R* model is such that the root-mean-square value of the field is 1 nG. In the two other scenarios the EGMF is of astrophysical origin. These two models are called *astrophysical* and *astrophysicalR*. In each of them the magnetic energy is assumed to be 50% of the injected thermal energy, and it is released as a dipole around the injection region. Emission occurs in halos where the physical gas number density exceed the critical value of $10^{-2}\,\mathrm{cm}^{-3}$. These EGMF models are shown in Figure 1 within a volume of 250 Mpc/h each side. We also consider two other configurations: the *No EGMF* scenario, where no EGMF is considered and the propagation is purely ballistic, and the *statistical* scenario, where the EGMF is a statistically uniform Kolmogorov-like power-law spectrum with root-mean-square field strength $B_{\mathrm{rms}} = 1\,\mathrm{nG}$, and coherence length $\lambda_c = 1\,\mathrm{Mpc}$. We recall that in the case of a statistically uniform magnetic field, the root-mean-square deflection angle is given by

$$\theta_{\mathrm{rms}}(E,d) \simeq 1^\circ \cdot Z \left(\frac{E}{10^{20}\,\mathrm{eV}}\right)^{-1} \left(\frac{d}{10\,\mathrm{Mpc}}\right)^{1/2} \left(\frac{\lambda_c}{1\,\mathrm{Mpc}}\right)^{1/2} \left(\frac{B_{\mathrm{rms}}}{1\,\mathrm{nG}}\right), \tag{1}$$

where Z and E are the charge number and the energy of the particle respectively, and d is the rectilinear propagated distance [8]. The latter two cases give us the opportunity to study the effects not only of the presence of an EGMF, but also of the presence of a more complex spatial magnetic configuration (e.g. clusters, filaments and voids).

3. CRPropa simulations

All the processes described in the previous section were considered in our UHECR propagation simulations. In this work we use the publicly available Monte Carlo code CRPropa3[1] [9]. With the CRPropa3 code, the Lorentz equation is numerically integrated in a three-dimensional volume, taking into account magnetic deflection, photohadronic interactions, redshift energy loss and nuclear decay. We simulate the propagation within a cubic volume of 250 Mpc/h each side. We define a periodic boundary condition such that if a cosmic ray leaves the volume, the trajectory is continued on the opposite side, and the initial injection position is changed accordingly. This means that each virtual replica of the volume will contain one spherical observer.

The simulation of a single event ends in two ways: if the energy becomes smaller than $8 \cdot 10^{18}$ eV, the event is not recorded and the simulation ends; if the event intersects the observer, represented by a sphere of radius 1 Mpc located in the center of the simulation volume, the particle is recorded and the simulation ends.

We define two source distribution models, both characterized by a source number density of $n_S \simeq 1.6 \cdot 10^{-4}\,\mathrm{Mpc}^{-3}\mathrm{h}^3$, which corresponds to a catalogue of 2500 point-like sources. In the *homogeneous* model, we obtain the catalogue with a homogeneous sampling of the positions in the simulation volume. We also consider a structured source distribution, called *density* model. In this scenario, the source catalogue is obtained with a sampling of the source positions with probability density proportional to the baryon density distribution reported in [7]. All the sources within one catalogue emit cosmic rays with the same rate. As for the EGMF models, the purpose of these two source models is to study the effect on the arrival directions of a structured source distribution.

The injection of two pure composition is considered: pure protons and pure irons. The initial energy is extracted following a power-law spectrum $dN/dE \propto E^{-1}$ between 8 EeV and 10^3 EeV, and the injected momentum is chosen isotropically. This energy spectrum does not correspond to a real physical spectrum. Due to the relation between the cosmic ray energy and the horizon effects, reweighing of observed events in order to reproduce realistic injection spectra could affect the results presented in the next section. We run simulations for 10 different realizations of each source catalogue, always requiring the observation of 10.000 events with $E \geq 8 \cdot 10^{18}$ eV. All the combinations of EGMF model, source catalogue and injected composition presented above are simulated.

We assume that our observer surface represents the border of the Milky Way halo. However, the GMF is $\sim 1 - 10\,\mu$G, so the magnetic deflection due to propagation in the galactic region can reach several degrees. In order to also reproduce this deflection, we apply magnetic lens to our observed UHECR to map the sky at the edge of the Galaxy, to the sky at Earth. In this work we use the JF12 model for the GMF [11] implemented in CRPropa3.

4. Analysis and results

The momentum vector of an observed event is recorded in the output file of the simulation. We use these vectors to compute the sky map distribution $\Phi(\hat{n})$ of the UHECR arrival directions (i.e. the probability density function of observing an UHECR from the direction $\hat{n}$). We use the

[1]Version 3.2 of CRPropa3 is used in this work.

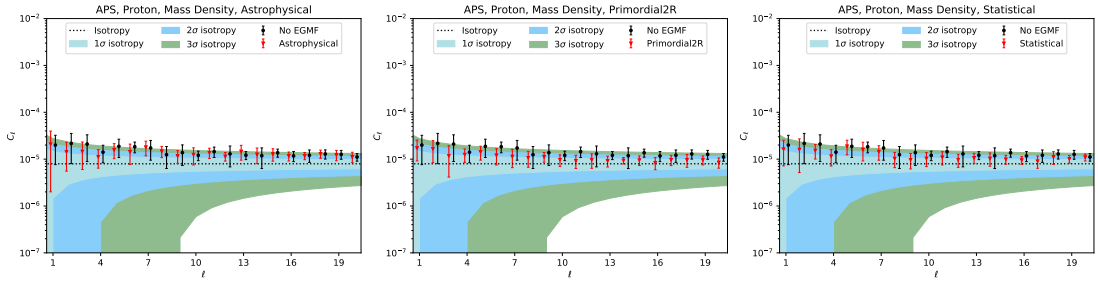

Figure 2: Angular power spectra at the observer for the recorded cosmic rays with $E \geq 8 \cdot 10^{18}$ eV. Pure proton injection and *density* source catalogue. Magnetic filed model from left to right: *astrophysical*, *primordial2R* and *statistical*. In each panel the isotropic prediction (4) (black dotted line and coloured areas), scenarios without magnetic filed (red circles) and with one magnetic field model (red triangles) are shown. The $1\sigma_l^{\rm iso}$, $2\sigma_l^{\rm iso}$ and $3\sigma_l^{\rm iso}$ areas are shown in cyan, blue and green, respectively. The mean values and the error bars represent the mean and cosmic variance, respectively.

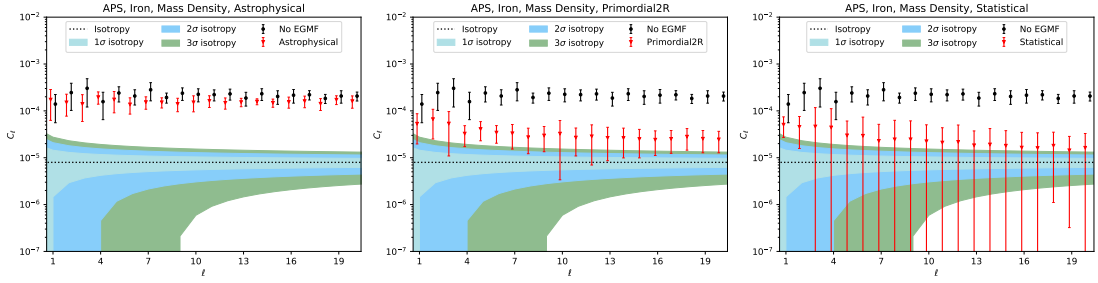

Figure 3: Same as Figure 2 for a pure iron injection.

Python package HEALPY [10], based on the Hierarchical Equal Area isoLatitude Pixelization (HEALPix[2]) scheme [12], for our spherical data analysis.

In order to evaluate the anisotropy level of the observed sky maps, the distributions $\Phi(\hat{n})$ have been decomposed in spherical harmonics

$$\Phi(\hat{n}) = \sum_{l=0}^{+\infty} \sum_{m=-l}^{l} a_{lm} Y_{lm}(\hat{n}) \,, \tag{2}$$

from which the Angular Power Spectrum (APS) C_l is computed as

$$C_l = \left\langle |a_{lm}|^2 \right\rangle = \frac{1}{2l+1} \sum_{m=-l}^{l} |a_{lm}|^2 \,. \tag{3}$$

We compute (3) by using the developed tools in HEALPY for the multipoles $l \leq 20$. For each combination of source model, EGMF and injected composition, we compute the C_l of the 10 realizations of the source catalogue. We then calculate the mean and cosmic variance. We compare the obtained APSs with the expected isotropic prediction with the same number of particles observed,

[2]https://healpix.sourceforge.io

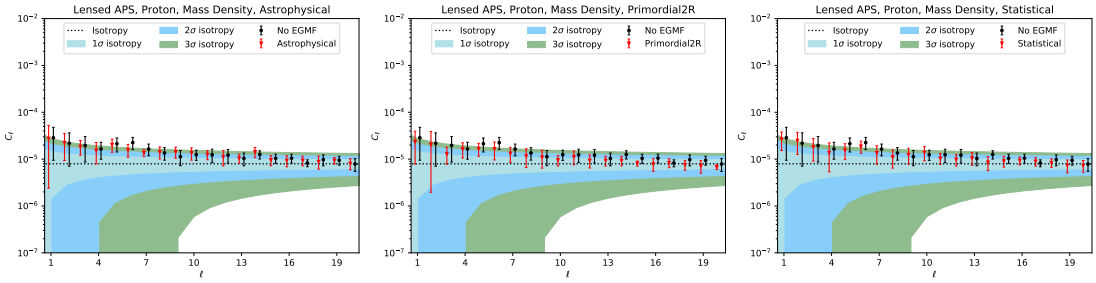

Figure 4: Same as Figure 2 applying the galactic lens.

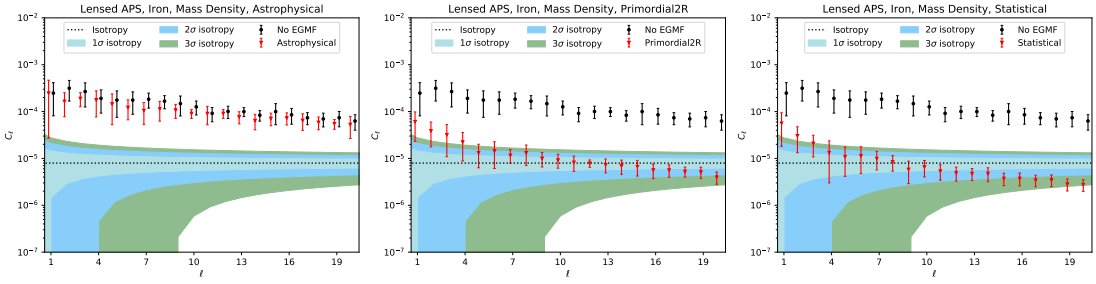

Figure 5: Same as Figure 3 applying the galactic lens.

given by

$$C_l^{\rm iso} = \frac{1}{4\pi N} \quad , \quad \sigma_l^{\rm iso} = \sqrt{\frac{2}{2l+1}} C_l^{\rm iso}, \tag{4}$$

where $N = 10.000$.

In Figure 2 we show the APSs for pure proton composition and *density* source distribution: the scenarios without EGMF (red circles) and with one EGMF model (red triangles) are shown together with the isotropic prediction (4) (black dotted line and coloured areas). The $1\sigma_l^{\rm iso}$, $2\sigma_l^{\rm iso}$ and $3\sigma_l^{\rm iso}$ areas are shown in cyan, blue and green, respectively. The APSs in the presence of EGMF are slightly lower than those without any EGMF. This result shows that the effect of the magnetic deflection is to slightly reduce the anisotropy level associated to the pure source distribution, although within the cosmic variance. However, all the C_l are marginally larger than the isotorpic prediction, but still within the $3\sigma_l^{\rm iso}$ area. Considering the *homogeneous* source catalogue, the observed angular power spectra are slightly lower than in the case of the *density* catalogue. This is due to the difference in the spatial distribution of the sources of the two catalogues. All results concerning the effect of the EGMFs shown in Figure 2 and 3 are also valid when the *homogeneous* source catalogue is used.

In Figure 3 the same quantities of Figure 2 are shown for pure iron injection. The APS for the case without EGMF is now shifted to higher values. This effect is due to the photodisintegration of heavy nuclei with CMB photons, which limits the observable source distance to $\sim 10\,$Mpc for $E \gtrsim 10^{20}\,$eV. The sky exhibits a more anisotropic behaviour, which reflects the distribution of very nearby sources. This is also evident by the fact that the C_l are bigger than $C_l^{\rm iso}$. The effect of the magnetic field is significantly accentuated in the case of heavy nuclei (as expected from the fact that the magnetic deflection depends on the charge number Z). The magnetic deflection spreads the

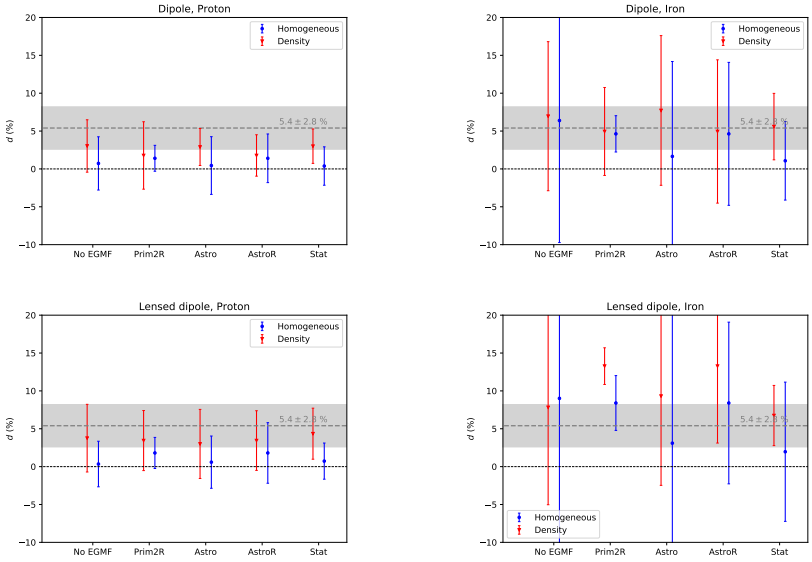

Figure 6: Dipole vector strength for all the configuration considered. Top left: proton injection. Top right: iron injection. Bottom left: proton injection applying the galactic lens. Bottom right: iron injection applying the galactic lens. The grey line and area represent the dipole value reported in [13].

arrival directions in the sky, consequently reducing the mean value of the APSs. It is clear that this magnetically-induced isostropization of the sky is more efficient as the average magnetization of the extragalactic space increases. Furthermore, the high-multipole components of the APSs ($l \gtrsim 5$) show greater sensitivity to the EGMF than low-multipoles (dipole and quadrupole).

As described in the previous section, we reproduce the propagation in the GMF by applying a magnetic lens to the observed UHECRs. The corresponding angular power spectra are shown in Figures 4 and 5. The effect of the galactic deflection is a general suppression of the high-multipole components for all the configurations described above. It can also be seen that low multipoles, such as dipole and quadrupole, are weakly affected by the GMF. These components still show a deviation from the isotropic prediction. We observe that the additional deflection due to the GMF is not able to suppress the effects of the EGMF. This suggests that a possible footprint of the EGMF could be observed in data measured at Earth.

We now want to evaluate the dipole contribution in the arrival direction distributions. To that end, we express the denity function $\Phi(\hat{n})$ as

$$\Phi(\hat{n}) = \Phi_0 \left(1 + \vec{d} \cdot \hat{n} + ...\right), \tag{5}$$

where Φ_0 is the average value of $\Phi(\hat{n})$ over the sky, and $\vec{d}$ is the dipole vector. The obtained dipole vector strengths d are shown in Figure 6 together with the value $d = 5.4 \pm 2.8\,\%$ reported in [13]. Several conclusions can be obtained from Figure 6. An homogeneous source distribution generally leads to a weaker dipole than a structured distribution, regardless of the magnetic field model adopted. This tells us that galactic and extragalactic deflections cannot completely suppress the signal due to the source distribution. On average, the highest dipole contributions come from the scenarios where the extragalactic space is less magnetized. This is due to the fact that strong

magnetic fields result in large deflection, which tends to isotropize the arrival directions distribution. The galactic deflection increases the dipole values, as predicted by the analysis of the angular power spectra. We observe different combinations of propagation models that could be compatible with observational data.

5. Conclusions

We simulated the propagation of UHECRs (in particular protons and iron nuclei) with the Monte Carlo code CRPropa3. We considered all the relevant photohadronic interactions, redshift energy loss and nuclear decay. We used realistic configurations of matter and magnetic field distributions of the local Universe, using MHD simulation results. We considered three structured EGMF models, one statistically homogeneous field and the case without magnetic field together with structured and homogeneous source catalogues. We reproduced the galactic deflection using the magnetic lensing technique.

From the study of the angular power spectrum, we observed that heavy nuclei deviate strongly from the isotropic prediction, due to both the interaction horizon and the magnetic deflection. Moreover, EGMFs can isotropize the observed UHECR sky deflecting during the propagation. This effect becomes gradually more intense as the magnetization of the extragalactic space increases. The GMF introduces a suppression of the high-multipole components of the APSs. The study of the observed dipole shows that this quantity is sensitive to both the source distribution and the EGMF model. As obtained for the APSs, a lower extragalactic magnetization corresponds to a stronger dipole signal.

Future developments of this work will include the study of more UHECR observables (e.g. energy spectrum and mass composition), and the investigation of other possible footprints of different EGMF models. Simulations of intermediate nuclear masses (He, N and Si) are being performed in order to be able to compare our simulated observables with real UHECR data.

References

[1] A. Aab *et al.* [Pierre Auger], Nucl. Instrum. Meth. A **798** (2015), 172-213.
[2] A. Aab *et al.* [Pierre Auger], Science **357** (2017) no.6537, 1266-1270.
[3] K. Greisen, Phys. Rev. Lett. **16** (1966), 748-750.
[4] G. T. Zatsepin and V. A. Kuzmin, JETP Lett. **4** (1966), 78-80.
[5] R. C. Gilmore *et al.*, Mon. Not. Roy. Astron. Soc. **422** (2012), 3189.
[6] G. L. Bryan *et al.* [ENZO], Astrophys. J. Suppl. **211** (2014), 19.
[7] S. Hackstein *et al.*, Mon. Not. Roy. Astron. Soc. **475** (2018) no.2, 2519-2529.
[8] E. Waxman and J. Miralda-Escude, Astrophys. J. Lett. **472** (1996), L89-L92.
[9] R. Alves Batista *et al.*, JCAP **09** (2022), 035.
[10] A. Zonca *et al.*, Journal of Open Source Software **4** (2019) no.35, 1298
[11] R. Jansson and G. R. Farrar, Astrophys. J. **757** (2012), 14.
[12] K. M. Górski *et al.*, Astrophys. J. **622** (2005), 759-771.
[13] A. Aab *et al.* [Pierre Auger], Astrophys. J. **868** (2018) no.1, 4.